# Luminescent Liquid Crystals Derived from 9,10-Bis(Phenylethynyl)anthracene

Raquel Giménez, Milagros Piñol, and José Luis Serrano*

*Química Orgánica, Facultad de Ciencias-ICMA, Universidad de Zaragoza-CSIC, 50009 Zaragoza (Spain)*

*Received July 31, 2003. Revised Manuscript Received January 30, 2004*

Liquid crystalline behavior has been found in a series of low-molecular-weight 9,10-disubstituted anthracenes. In particular, nematic mesomorphism is displayed by derivatives bearing at least a 4′-pentylbiphenyl-4-ylethynyl group, showing that the presence of this substituent induces a mesophase despite the broad central core of the anthracene skeleton. These compounds can also be seen as derived from the known fluorescent material 9,10-bis(phenylethynyl)anthracene (BPEA) with a *p*-pentylphenyl substituent (among others) along its long axis. A comparison of the optical properties of the compounds relative to the parent compound BPEA is presented in order to evaluate their applications in emissive devices. A study of a nematic compound in solution, PMMA film, and pure state in the different phases shows high fluorescence in solution in the green region that slightly shifts to higher wavelengths in PMMA films, but it is clearly red-shifted in pure state.

## 1. Introduction

The search for new liquid crystals is a productive area of research in materials chemistry that has been powered by many discoveries of technological and valuable commercial applications for display devices, light modulators, thermography, etc.[1] Functional materials can be obtained by furthering the self-organization of liquid crystals incorporating other properties in the same molecule such as luminescence. This combination in particular has led to intrinsically luminescent mesogens,[2−4] which are emitters that in pure state could lead to ordered aggregates with large carrier mobilities for EL devices.[5] In mixtures, their anisotropy has improved compatibility with liquid crystalline or polymeric matrixes and they have shown higher orientational ability than isotropic emitters involving important applications in polarized luminiscence for emissive displays.[6]

Among fluorescent materials, anthracene derivatives and, in particular, 9,10-disubstituted compounds (also called mesosubstituted) such as 9,10-diphenylanthracene and 9,10-bis(phenylethynyl)anthracene (BPEA) are some of the strongest fluorophores known.[7] BPEA and derivatives emit in the green region and are used in chemiluminescent formulations[8] and as molecular probes[9] and have been studied for OLED[10] and PLED[11] devices.

* To whom correspondence should be addressed. E-mail: joseluis@unizar.es. Fax and phone: (+)34 976 761209.

(1) Demus, D., Goodby, J., Gray, G. W., Spiess, H.-W., Vill, V., Eds.; *Handbook of Liquid Crystals*; Wiley-VCH: Weinheim, 1998; vol. 1, ch. IX, p 731.

(2) Examples of rodlike intrinsically luminescent LC. (a) Subramanian, R.; Patterson, L. K.; Levanon, H. *Chem. Phys. Lett.* **1982**, *93*, 578. (b) David, C.; Baeyens-Volant, D. *Mol. Cryst. Liq. Cryst.* **1984**, *106*, 45. (c) Bubel, O. N.; Bezborodov, U. S.; Rachkevich, V. S. *Zh. Org. Khim.* **1982**, *18*, 1240. (d) Ikeda, T.; Kuhihara, S.; Tazuke, S. *J. Phys. Chem.* **1990**, *94*, 6550. (e) Chudgar, N. K.; Parekh, M. K., Madhavrao, S. S.; Sharma, H. C. *Liq. Cryst.* **1995**, *19*, 807. (f) Gill, R. E.; Meetsma, A.; Hadziioannou, G. *Adv. Mater.* **1996**, *8*, 212. (g) Davey, A. P.; Howard, R. G.; Blau, W. J. *J. Mater. Chem.* **1997**, *7*, 417. (h) Strehmel, B.; Sarker, A. M.; Malpert, J. H.; Strehmel, V.; Seifert, H.; Neckers, D. C. *J. Am. Chem. Soc.* **1999**, *121*, 1226. (i) Kim, S.; Park, S. Y. *Mol. Cryst. Liq. Cryst., Sect. A* **1999**, *337*, 405. (j) Bacher, A.; Bentley, P. G.; Bradley, D. D. C.; Douglas, L. K.; Glarvey, P. A.; Grell, M.; Whitehead, K. S.; Turner, M. L. *J. Mater. Chem.* **1999**, *9*, 2985. (k) Attias, A.-J.; Cavalli, C.; Bloch, B.; Guillou, N.; Noël, C. *Chem. Mater.* **1999**, *11*, 2057. (l) Attias, A.-J.; Hapiot, P.; Wintgens, V.; Valat, P. *Chem. Mater.* **2000**, *12*, 461. (m) Sumiyoshi, T.; Takahashi, I.; Tsuboi, Y.; Miyasaka, H.; Itaya, A.; Asahi, T.; Masuhara, H. *Thin Solid Films* **2000**, *370*, 285. (n) Oriol, L.; Piñol, M.; Serrano, J. L.; Martínez, C.; Alcalá, R.; Cases, R.; Sánchez, C. *Polymer* **2001**, *42*, 2737. (o) Sentman, A. C.; Gin, D. L. *Adv. Mater.* **2001**, *13* (18), 1398. (p) Sato, N.; Ishii, R.; Nakashima, S.; Yonetake, K.; Kido, J. *Liq. Cryst.* **2001**, *28*, 1211. (q) Schenning, A. P. H. J.; Kilbinger, A. F. M.; Biscarini, F.; Cavallini, M.; Cooper, H. J.; Derrick, P. J.; Feast, W. J.; Lazzaroni, R.; Leclere, Ph.; McDonell, L. A.; Meijer, E. W.; Meskers, S. C. J. *J. Am. Chem. Soc.* **2002**, *124*, 1269. (r) Millaruelo, M.; Oriol, L.; Piñol, M.; Sáez, P. L.; Serrano, J. L. *J. Photochem. Photobiol. A* **2003**, *155*, 29. (s) Haristoy, D.; Tsiourvas, D. *Chem. Mater.* **2003**, *15*, 2079.

(3) Examples of fluorescent phasmidic liquid crystals: (a) Hoag, B. P.; Gin, D. L. *Adv. Mater.* **1998**, *10*, 1546. (b) Levitsky, I. A.; Kishikawa, K.; Eichhorn, S. M.; Swager, T. M. *J. Am. Chem. Soc.* **2000**, *122*, 2474.

(4) Disklike: (a) Ecoffet, C.; Markovitsi, D.; Jallabert, C.; Strzelecka, H.; Veber, M. *Thin Solid Films* **1994**, *242*, 83. (b) Marguet, S.; Markovitsi, D.; Goldmann, D.; Janietz, D.; Praefcke, K.; Singer, D. *J. Chem. Soc., Faraday Trans.* **1997**, *93*, 147. (c) Cormier, R. A.; Gregg, B. A. *Chem. Mater.* **1998**, *10*, 1309. (d) Rohr, U.; Schlichting, P.; Böhm, A.; Gross, M.; Meerholz, K.; Bräuchle, C.; Müllen, K. *Angew. Chem., Int. Ed.* **1998**, *37*, 1434. (e) Ito, S.; Herwig, P. T.; Böhme, T.; Rabe, J. P.; Rettig, W.; Müllen, K. *J. Am. Chem. Soc.* **2000**, *122*, 7698. (f) Benning, S.; Kitzerow, H.-S.; Bock, H.; Achard, M.-F. *Liq. Cryst.* **2000**, *27*, 901. (g) Benning, S. A.; Hassheider, T.; Keuker-Bauman, S.; Bock, H.; Salla, F. D.; Frauenheim, T.; Kitzerow, H.-S. *Liq. Cryst.* **2001**, *28*, 1105. (h) Attias, A.-J.; Cavalli, C.; Donnio, B.; Guillon, D.; Hapiot, P.; Malthête, J. *Chem. Mater.* **2002**, *14*, 375.

(5) (a) Adam, D.; Schuhmacher, P.; Simmerer, J.; Häussling, L.; Siemensmeyer, K.; Etzbach, K. H.; Ringsdorf, H.; Haarer, D. *Nature* **1994**, *371*, 141. (b) For a review see Lüssem, G.; Wendorff, J. H. *Polym. Adv. Technol.* **1998**, *9*, 443.

(6) (a) Grell, M.; Bradley, D. D. C. *Adv. Mater.* **1999**, *11*, 895 and refs therein. (b) Eglin, M.; Montali, A.; Palmans, A. R. A.; Tervoort, T.; Smith, P.; Weder, Ch. *J. Mater. Chem.* **1999**, *9*, 2221. (c) Palmans, A. R. A.; Eglin, M.; Montali, A.; Weder, C.; Smith, P. *Chem. Mater.* **2000**, *12*, 472.

(7) (a) Furst, M.; Kallman, H.; Brown, F. H. *J. Chem. Phys.* **1957**, *26*, 1321. (b) Zweig, A.; Maurer, A. H.; Roberts, B. G. *J. Org. Chem.* **1967**, *32*, 1322. (c) Maulding, D. R.; Roberts, B. G. *J. Org. Chem.* **1969**, *34*, 1734. (d) Heller, C. A.; Henry, R. A.; McLaughlin, B. A.; Bliss, D. E. *J. Chem. Eng. Data* **1974**, *19*, 214.

10.1021/cm030582u CCC: $27.50 
Published on Web 03/11/2004

**Scheme 1**

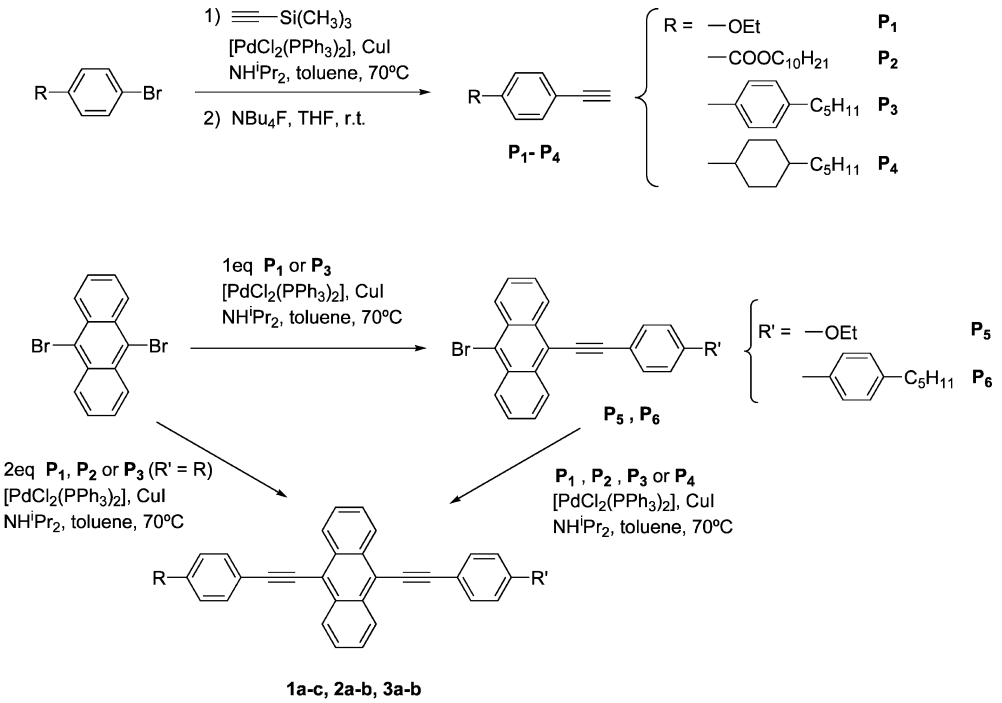


| R | R' | Compound |
|---|---|---|
| —OEt | —OEt | 1a |
| —OEt | —$COOC_{10}H_{21}$ | 1b |
| —$COOC_{10}H_{21}$ | —$COOC_{10}H_{21}$ | 1c |
| —$C_5H_{11}$ | —OEt | 2a |
| —$C_5H_{11}$ | —$COOC_{10}H_{21}$ | 2b |
| —$C_5H_{11}$ | —$C_5H_{11}$ | 3a |
| —$C_5H_{11}$ | —$C_5H_{11}$ | 3b |

Although polarized luminescence can be obtained with BPEA itself, we are interested in the elongation of the BPEA core along the long axis of the chromophore (that is the 9,10 position of the anthracene) for two reasons. First, to generate materials with the same or improved luminescent properties but with better dichroic properties, as it is known that the transition moment of the longest wavelength absorption is polarized parallel to the long axis.[12] Second, to induce mesomorphic behavior and therefore more compatible materials with LC mixtures or LC polymers as a way to uniaxially align the emitting dyes.

In this work we present the modifications conducted on the BPEA core to induce mesomorphic behavior despite the broad central core of the anthracene skeleton. All the compounds prepared are shown in Scheme 1. They are 9,10-bis(phenylethynyl)anthracenes with aliphatic (ethoxy or decyloxycarbonyl), aromatic (*p*-pentylphenyl), or alicyclic (*trans*-4-pentylcyclohexyl) R and R′ groups.

## 2. Experimental Section

**2.1 Materials and Techniques.** 4-Bromo-4′-*n*-pentylbiphenyl, 1-bromo-4-(*trans*-4′-*n*-pentylcyclohexyl)benzene, and *p*-ethoxyphenylacetylene (**P1**) were supplied by Merck. 9,10-

(8) (a) Maulding, D. R.; Zweig, A. U.S. Patent 3729426, 1973. b) Gill, S. K. *Aldrichimica Acta* **1983**, *16*, 59. (c) Hanhela, P. J.; Paul, D. B. *Aust. J. Chem*. **1984**, *37*, 553. (d) Nakatsuji, S.; Matsuda, K.; Uesugi, Y.; Nakashima, K.; Akiyama, S.; Fabian, W. *J. Chem. Soc., Perkin Trans. 1* **1992**, 755. (e) Li, B.; Miao, W.; Cheng, L. *Dyes Pigm*. **2000**, *46*, 81.

(9) See for example: Cicerone, M. T.; Blackburn, F. R.; Ediger, M. D. *J. Chem. Phys.* **1995**, *102*, 47.

(10) Ishibashi, T. Eur. Pat. Appl. EP 1072668 A2 31, 2001.

(11) (a) Swager, T. M.; Gil, D. J.; Wrighton, M. S. *J. Phys. Chem*. **1995**, *99*, 4886. (b) Ofer, D.; Swager, T. M.; Wrighton, M. S. *Chem. Mater*. **1995**, *7*, 418.

(12) Levitus, M.; García-Garibay, M. A. *J. Phys. Chem. A* **2000**, *104*, 8632.

Bis(phenylethynyl)anthracene, trimethylsilylacetylene, dichlorobis(triphenylphosphine)palladium(II), copper(I) iodide, tetrabutylammonium fluoride hydrate, 9,10-dibromoanthracene, dry toluene, and dry diisopropylamine were purchased from Aldrich and used without further purification; *n*-decyl *p*-bromobenzoate was prepared from *p*-bromobenzoic acid and *n*-decanol (Aldrich) as described in the literature.[13] All reactions were carried out under an argon atmosphere using Schlenk techniques and dry solvents. Infrared spectra were obtained with a Mattson Genesis (FTIR) or a ThermoNicolet spectrophotometer in the range $\nu = 400-4000$ cm$^{-1}$. $^1$H NMR and $^{13}$C NMR spectra were recorded on a Varian Unity 300 MHz spectrometer. Mass spectra were obtained with a VG Autospec spectrometer using 3-nitrobenzyl alcohol as matrix for positive FAB-LSIMS. The optical textures of the mesophases were studied with an Olympus polarizing microscope equipped with a Linkam THMS600 hot stage. The transition temperatures and enthalpies were measured by differential scanning calorimetry with a TA instruments apparatus operating at a scanning rate of 10 °C min$^{-1}$ on heating and calibrated with indium (156.6 °C; 28.4 J g$^{-1}$) as the standard. Absorption spectra were obtained with a Unicam spectrophotometer using spectroscopic grade solvents in quartz twin cells for solutions or quartz plates for solids or films. Films were prepared by drop casting a chloroform solution of 1% w/w of **2b** in PMMA (Aldrich, MW 120 000) onto quartz coverslips. Fluorescence studies were conducted with a Perkin-Elmer LS50B fluorometer. Quantum yields were measured relative to BPEA with an excitation wavelength of 440 nm from corrected emission spectra. Spectra of the films and the various phases of **2b** were recorded by front-face detection. The pure compound was introduced in a 5-$\mu$m Linkam cell from the isotropic liquid with the temperature of the sample controlled by a Linkam HTMS600 hotstage.

**2.2 General Procedure for the Synthesis of the Acetylene Derivatives ($\mathbf{P_2}-\mathbf{P_4}$).** To a Schlenk charged with 16.5 mmol of the bromo derivative (*n*-decyl *p*-bromobenzoate, 4-bromo-4′-*n*-pentylbiphenyl, or 1-bromo-4-(*trans*-4′-*n*-pentylcyclohexyl)benzene), 63 mg (0.33 mmol) of copper(I) iodide, and 116 mg (0.16 mmol) of dichlorobis(triphenylphosphine)-palladium(II) in 50 mL of dry toluene, was added 3 mL of dry diisopropylamine and 3 mL (21.2 mmol) of trimethylsilylacetylene dropwise. The mixture was stirred at 70 °C for 2 days under an Ar atmosphere. Afterward, the diisopropylamine was evaporated at the vacuum line and the toluene suspension was filtered through a pad of silicagel. The solvent was evaporated and the residue was dissolved in 100 mL of THF. Then, 4.31 g (16.5 mmol) of tetrabutylammonium fluoride hydrate were added and the reaction was stirred for 30 min at r.t. Afterward, 200 mL of water and 100 mL of diethyl ether were added and the organic layer was separated out and dried over magnesium sulfate, filtered, and evaporated. The residue was purified by column chromatography using hexane/dichloromethane 5:1 (for $\mathbf{P_2}$) or hexane (for $\mathbf{P_3}$ and $\mathbf{P_4}$) as eluent. Yield: 60−65%.

**$\mathbf{P_2}$.** Light yellow liquid. IR (Nujol, NaCl) $\nu = 3302, 3258, 2108, 1722, 1607, 1274, 858, 769$. $^1$H NMR (300 MHz, $CDCl_3$) $\delta = 0.86$ (t, $J = 6.0$ Hz, 3H), 1.25−1.41 (m, 14H), 1.71−1.76 (m, 2H), 3.20 (s, 1H), 4.29 (t, $J = 6.9$ Hz, 2H), 7.52 (d, $J = 8.4$ Hz, 2H), 7.98 (d, $J = 8.4$ Hz, 2H).

**$\mathbf{P_3}$.** White solid. mp 80 °C. IR (Nujol, NaCl) $\nu = 3275, 2108, 1491, 835, 813$. $^1$H NMR (300 MHz, $CDCl_3$) $\delta = 0.89$ (t, $J = 6.8$ Hz, 3H), 1.31−1.36 (m, 4H), 1.61−1.66 (m, 2H), 2.63 (t, $J = 6.5$ Hz, 2H), 3.11 (s, 1H), 7.25 (d, $J = 8.3$ Hz, 2H), 7.49 (d, $J = 8.0$ Hz, 2H), 7.54 ("s", 4H).

**$\mathbf{P_4}$.** White solid. mp 37 °C. IR (Nujol, NaCl) $\nu = 3316, 2108, 1509, 832$. $^1$H NMR (300 MHz, $CDCl_3$) $\delta = 0.88$ (t, $J = 6.2$ Hz, 3H), 0.92−1.08 (m, 2H), 1.21−1.34 (m, 9H), 1.38−1.49 (m, 2H), 1.84 ("d", $J = 11$ Hz, 4H), 2.44 (tt, $J = 11$ Hz, $J = 1.7$ Hz, 1H), 3.00 (s, 1H), 7.14 (d, $J = 8.0$ Hz, 2H), 7.39 (d, $J = 8.0$ Hz, 2H).

**2.3 Procedure for the Synthesis of the Anthracene Derivatives.** Symmetrically and nonsymmetrically substituted compounds have been prepared by reaction of 9,10-dibromoanthracene with the acetylene derivatives ($\mathbf{P_1}-\mathbf{P_4}$) using adapted Sonogashira coupling reactions[14] in one or two steps (Scheme 1). The reactions proceeded slower than the reported coupling to 9,10-diiodoanthracene[15] but heating at 70 °C for 12−24 h obtained the desired compounds with moderate to good yields as crystals ranging from yellow to red. In particular, compounds **1b**, **1c**, **2b**, and **3b** could be isolated from the purification procedure following nonreproducible procedures of recrystallization or evaporation, or after a thermal process, as crystals of two different colors that could be studied separately (see below).

*General Synthesis of the Monocoupled Compounds (**P5** and **P6**).* To a Schlenk charged with 5.5 g (16.5 mmol) of 9,10-dibromoanthracene, 63 mg (0.33 mmol) of copper(I) iodide, 116 mg (0.165 mmol) of dichlorobis(triphenylphosphine)palladium-(II), 300 mL of dry toluene, and 3.5 mL of dry diisopropylamine at 70 °C, was added dropwise a solution of 18.14 mmol of acetylene derivative $\mathbf{P_1}$ or $\mathbf{P_3}$ in 30 mL of toluene. The addition was carried out via an addition funnel over 12 h. The reaction mixture was stirred for 1 day at 70 °C under argon, after which it was evaporated to dryness and the crude was purified by column chromatography using first hexane and second a mixture of hexane/dichloromethane 10:1. Yield: 25−35%.

**$\mathbf{P_5}$.** Yellow solid. mp 158 °C. IR (Nujol, NaCl) $\nu = 2200, 1599, 1508, 1252$. $^1$H NMR (300 MHz, $CDCl_3$) $\delta = 1.44$ (t, $J = 7$ Hz, 3H), 4.08 (q, $J = 7$ Hz, 2H), 6.94 (d, $J = 8.8$ Hz, 2H), 7.57−7.65 (m, 4H), 7.67 (d, $J = 8.8$ Hz, 2H), 8.52−8.55 (m, 4H), 8.65−8.69 (m, 4H).

**$\mathbf{P_6}$.** Yellow solid. mp 166 °C. IR (Nujol, NaCl) $\nu = 1492, 753$. $^1$H NMR (300 MHz, $CDCl_3$) $\delta = 0.89$ (t, $J = 6.6$ Hz, 3H), 1.25−1.39 (m, 4H), 1.65−1.67 (m, 2H), 2.67 (t, $J = 7.5$ Hz, 2H), 7.30 (d, $J = 8.0$ Hz, 2H), 7.57−7.70 (m, 8H), 7.82 (d, $J = 8.0$ Hz, 2H), 8.56−8.59 (m, 2H), 8.70−8.74 (m, 2H).

*General Synthesis for the Nonsymmetric Compounds (**1b**, **2a**, **2b**, **3b**).* To a Schlenk charged with 800 mg (1.6 mmol) of monocoupled compound ($\mathbf{P_5}$ or $\mathbf{P_6}$), 6 mg (0.032 mmol) of copper(I) iodide, 11 mg (0.016 mmol) of dichlorobis(triphenylphosphine)palladium(II), 30 mL of dry toluene, and 0.3 mL of dry diisopropylamine at 70 °C, is added dropwise a solution of 1.7 mmol of the acetylene derivative ($\mathbf{P_1}-\mathbf{P_4}$) in 30 mL of toluene. The reaction mixture is heated at 70 °C for 24 h, filtered though a pad of Celite, and evaporated to dryness. The residue was purified by column chromatography using hexane/dichloromethane 9:1 and recrystallized in hexane or hexane/dichloromethane. Yield: 75−85%.

*General Synthesis for the Symmetric Compounds (**1a**, **1c**, **3a**).* To a Schlenk charged with 1 g (2.97 mmol) of 9,10-dibromoanthracene, 23 mg (0.12 mmol) of copper(I) iodide, 42 mg (0.06 mmol) of dichlorobis(triphenylphosphine)palladium-(II), 50 mL of dry toluene, and 1.5 mL of dry diisopropylamine at 70 °C, was added dropwise a solution of 6.53 mmol of acetylene derivative ($\mathbf{P_1}-\mathbf{P_3}$) in 10 mL of toluene. The reaction mixture was stirred for 1 day at 70 °C under argon, after which it was evaporated to dryness and the crude was purified by column chromatography using first hexane and second a mixture of hexane/dichloromethane 3:2. Finally it was recrystallized in hexane or in a mixture of hexane/dichloromethane. Yield: 40−60%.

**2.4 Characterization Data for the BPEA Derivatives.**
**1a.** Yellow crystals. IR (KBr) $\nu = 3056$ (Car−H), 2977, 2930, 2897, 2884, 2878 (C−H), 2196 (C≡C), 1714 (OC═O), 1601, 1509 (C═Car), 1249 (C−O). $^1$H NMR (300 MHz, $CDCl_3$) $\delta = 1.45$ (t, $J = 7$ Hz, 6H), 4.09 (q, $J = 7$ Hz, 4H), 6.94 (d, $J = 8.8$ Hz, 4H), 7.60 (m, 4H), 7.68 (d, $J = 8.8$ Hz, 4H), 8.66 (m, 4H). MS (LSIMS): 466 [$M^+$], 439. Anal. Calcd. for $C_{34}H_{26}O_2$: C, 87.52; H, 5.62. Found: C, 87.48; H, 5.58.

**1b.** Yellow crystals (C): IR (KBr) $\nu = 3051$ (Car−H), 2961, 2923, 2851 (C−H), 2184 (C≡C), 1719 (OC═O), 1603, 1510

(13) Shinohara, K.-I.; Kato, F.; Minami, H.; Higuchi, H. *Polymer* **2001**, *42*, 8483.

(14) (a) Sonogashira, K.; Toda, Y.; Hagihara, N. *Tetrahedron Lett.* **1975**, 4467. (b) Takahashi, S.; Yuroyama, Y.; Sonogashira, K.; Hagihara, N. *Synthesis* **1980**, 627.

(15) Nguyen, P.; Todd, S.; van den Biggelaar, D.; Taylor, N. J.; Marder, T. B.; Wittmann, F.; Friend, R. H. *Synlett* **1994**, 299.

(C═Car), 1278, 1253 (C−O). Red crystals (C′): IR (KBr) $\nu$ = 3050 (Car−H), 2958, 2922, 2848 (C−H), 2184 (C≡C), 1708 (OC═O), 1602, 1509 (C═Car), 1277, 1248 (C−O). $^1$H NMR (300 MHz, $CDCl_3$) $\delta$ = 0.87 (t, $J$ = 6.9 Hz, 3H), 1.27−1.40 (m, 14H), 1.45 (t, $J$ = 6.9 Hz, 3H), 1.79 (m, 24H), 4.09 (q, $J$ = 6.9 Hz, 2H), 4.34 (t, $J$ = 6.6 Hz, 2H), 6.95 (d, $J$ = 8.7 Hz, 2H), 7.63 (m, 4H), 7.69 (d, $J$ = 8.7 Hz, 2H), 7.80 (d, $J$ = 8.7 Hz, 2H), 8.10 (d, $J$ = 8.7 Hz, 2H), 8.65−8.68 (m, 4H). MS (LSIMS): 606 (100) [$M^+$]. Anal. Calcd. for $C_{43}H_{42}O_3$: C, 85.11; H, 6.98. Found: C, 85.01; H, 6.88.

**1c.** Red crystals (C): IR (KBr) $\nu$ = 3058 (Car−H), 2948, 2919, 2848 (C−H), 2200 (C≡C), 1721 (OC═O), 1602 (C═Car), 1267 (C−O). Yellow crystals (C′): IR (KBr)) $\nu$ = 3053 (Car−H), 2952, 2918, 2848 (C−H), 2192 (C≡C), 1717 (OC═O), 1602 (C═Car), 1278, 1271 (C−O). $^1$H NMR (300 MHz, $CDCl_3$) $\delta$ = 0.87 (t, $J$ = 6.6 Hz, 6H), 1.27−1.46 (m, 28H), 1.79 (m, 4H), 4.34 (t, $J$ = 6.6 Hz, 4H), 7.64−7.68 (m, 4H), 7.81 (d, $J$ = 8.1 Hz, 4H), 8.11 (d, $J$ = 8.1 Hz, 4H), 8.65−8.68 (m, 4H). MS (LSIMS): 747 [$M^+$ + 1], 607. Anal. Calcd. for $C_{52}H_{58}O_4$: C, 83.61; H, 7.83. Found: C, 83.56; H, 7.80.

**2a.** Orange crystals. IR (KBr) $\nu$ = 3056 (Car−H), 2924, 2850 (C−H), 2181 (C≡C), 1600, 1508 (C═Car), 1248 (C−O). $^1$H NMR (300 MHz, $CDCl_3$) $\delta$ = 0.89 (t, 3H), 1.32−1.37 (m, 4H), 1.45 (t, $J$ = 7 Hz, 3H), 1.63−1.65 (m, 2H), 2.65 (t, $J$ = 7.5 Hz, 2H), 4.09 (q, $J$ = 7 Hz, 2H), 6.95 (d, $J$ = 8.8 Hz, 2H), 7.28 (d, $J$ = 8.1 Hz, 2H), 7.56 (d, $J$ = 8.1 Hz, 2H), 7.59−7.70 (m, 10H), 7.81 (d, $J$ = 8.4 Hz, 2H), 8.67−8.71 (m, 4H). MS (LSIMS): 568 [$M^+$]. Anal. Calcd. for $C_{43}H_{36}O$: C, 90.81; H, 6.38. Found: C, 90.77; H, 6.35.

**2b.** Yellow crystals (C): IR (KBr) $\nu$ = 3057 (Car−H), 2950, 2920, 2850 (C−H), 2193 (C≡C), 1713 (OC═O), 1602 (C═Car), 1274 (C−O). Orange crystals (C′): IR (KBr) $\nu$ = 3057 (Car−H), 2921, 2850 (C−H), 2194, 2184 (C≡C), 1721 (OC═O), 1602 (C═Car), 1271 (C−O). $^1$H NMR (300 MHz, $CDCl_3$) $\delta$ = 0.85−0.90 (m, 6H), 1.27−1.45 (m, 18H), 1.63−1.65 (m, *2*H), 1.76−1.81 (m, 2H), 2.65 (t, $J$ = 7.6 Hz, 2H), 4.34 (t, $J$ = 6.5 Hz, 2H), 7.28 (d, $J$ = 7.9 Hz, 2H), 7.57 (d, $J$ = 7.9 Hz, 2H), 7.82 (d, 4H), 8.11 (d, $J$ = 8.2 Hz, 2H), 8.64−8.73 (m, 4H). $^{13}$C NMR (75 MHz, $CDCl_3$) $\delta$ = 14.0, 14.1, 22.6, 22.7, 26.0, 28.7, 29.3, 29.5, 31.1, 31.5, 31.9, 35.6, 65.4, 87.0, 89.4, 101.5, 102.9, 117.6, 119.3, 121.8, 126.8, 126.9, 127.0, 127.1, 127.4, 127.9, 128.6, 129.0, 129.7, 130.2, 131.5, 132.0, 132.1, 132.2, 137.6, 141.5, 142.8, 166.1. MS (LSIMS): 708 [$M^+$]. Anal. Calcd. for $C_{52}H_{52}O_2$: C, 88.09; H, 7.39. Found: C, 87.98; H, 7.34.

**3a.** Dark orange crystals. IR (KBr) $\nu$ = 3051 (Car−H), 2943, 2923, 2852 (C−H), 2190 (C≡C), 1493 (C═Car). $^1$H NMR (300 MHz, $CDCl_3$) $\delta$ = 0.90 (t, $J$ = 6.6 Hz, 6H), 1.32−1.37 (m, 8H), 1.63−1.68 (m, 4H), 2.65 (t, $J$ = 7.7 Hz, 4H), 7.28 (d, $J$ = 8.1 Hz, 4H), 7.63−7.69 (m, 12H), 7.82 (d, $J$ = 8.1 Hz, 4H), 8.69−8.72 (dd, $J$ = 6.6 Hz, $J$ = 3.3 Hz, 4H). MS (LSIMS): 670 [$M^+$], 662, 647. Anal. Calcd. for $C_{52}H_{46}$: C, 93.09; H, 6.91. Found: C, 92.98; H, 6.88.

**3b.** Yellow-orange crystals (C): IR (KBr) $\nu$ = 3050 (Car−H), 2954, 2920, 2847 (C−H), 2196, 2184 (C≡C), 1493 (C═Car). Red-brown crystals (C′): IR (KBr) $\nu$ = 3051 (Car−H), 2954, 2923, 2850 (C−H), 2185 (C≡C), 1494 (C═Car). $^1$H NMR (300 MHz, $CDCl_3$) $\delta$ = 0.89 (m, 6H), 1.00−1.12 (m, 2H), 1.23−1.47 (m, 15H), 1.58−1.70 (m, 2H), 1.83−1.94 (m, 4H), 2.50 (tt, $J$ = 10.5 Hz, $J$ = 2.7 Hz, 1H), 2.62 (t, $J$ = 7.7 Hz, 2H), 7.25 (d, $J$ = 8.1 Hz, 4H), 7.56 (d, $J$ = 8.1 Hz, 2H), 7.59−7.69 (m, 8H), 7.81 (d, $J$ = 8.1 Hz, 2H), 7.59−7.69 (m, 8H), 7.81 (d, $J$ = 8.1 Hz, 2H), 8.67−8.71 (m, 4H). MS (LSIMS): 676 [$M^+$]. Anal. Calcd. for $C_{52}H_{52}$: C, 92.26; H, 7.74. Found: C, 92.21; H, 7.68.

## 3. Results and Discussion

**3.1 Liquid Crystalline Properties.** The thermal behavior of the compounds was investigated by polarized light microscopy and DSC. Data are gathered in Table 1. To our knowledge this is the first time that mesomorphism has been reported for BPEA derivatives.

The BPEA core per se or with small substituents R, R′ is not liquid crystalline because of its low length-to-breadth ratio. The anthracene core disrupts the rodlike molecular profile with respect to analogous tolanes for which nematic and smectic phases have been found.[6c,16] For this work compound **1a** with two ethoxy substituents was prepared and it melts directly to isotropic liquid. Other derivatives with small substituents such as R = R′ = Me, OMe, SMe, $N(Me)_2$, $N(Et)_2$, $CF_3$, CN, $NO_2$, Cl and R = OMe, R′ = $NO_2$, have been previously described and no mesomorphism has been reported.[8d,15] An increase of the length of the molecule with a long chain substituent like decyloxycarbonyl (compound **1b**) leads to the induction of a monotropic nematic phase as well as to a significant decrease of the melting point. Moreover, on cooling, this compound was obtained as a mixture of two crystalline forms that melt directly to the isotropic liquid at different temperatures and are visible by eye because of their different colors (yellow and red-orange, with the red form of higher melting point than the yellow).

**Table 1. Optical, Thermal, and Thermodynamic Data of the BPEA Derivatives**

| compound | DSC T/°C ($\Delta H$/ kJ mol$^{-1}$) |
|---|---|
| **1a** | C 252 (61.8) I (Dec) |
| **1b** | C 125 (48.6) I |
| | I 117[a] N 110 (41.6) C+C′ |
| | C 123 (21.3) I |
| | C′ 131 (14.7) I |
| **1c** | C 104 (18.8) C′ 132 (63.4) I |
| | I 119 (59.9) C′ |
| | C′ 131 (59.6) I |
| **2a** | C 191 (12.6) N 260 Dec |
| **2b** | C 130 (22.5) C′ 147 (36.3) N 209 (0.3) I |
| | I 208[a] N 125 (9.0) C″ 102 (16.3) C′ |
| | C′ 146 (24.8) N 208[a] I |
| **3a** | C 241 (37.8) N 270 Dec |
| **3b** | C 126 (13.2) C′ 255 (34.5) N 275 (165.5) Dec[b] |

[a] Transition only detected by optical microscopy. [b] Exothermic peak, the fluid sample transforms into a black solid.

However, compound **1c** with two decyloxycarbonyl groups is not liquid crystal although it shows a melting point similar to that of **1b**. The higher symmetry of the former favors the organization in the solid state and this fact may frustrate the appearance of the nematic phase. In the first heating cycle of **1c** two polymorphs of different color are also detected. The low-temperature crystals are red, and on heating over 104 °C they transform into yellow crystals which melt at 132 °C. On cooling the isotropic liquid the yellow form crystallizes and remains in this phase at room temperature, but it slowly transforms to the more thermodynamically stable red polymorph (Figure 1a).

Compounds of series **2** with a *p*-pentylphenyl substituent are enantiotropic liquid crystals. Elongation of the molecule with one aromatic ring with respect to series **1** induces the appearance of a nematic phase over a fairly large range of temperatures by favoring the intermolecular interactions along the long axis and minimizing the hindrance due to the broadening of the

(16) (a) Malthête, J.; Leclercq, M.; Dvolaitzky, M.; Gabard, J.; Billard, J.; Pontikis, V.; Jacques, J. *Mol. Cryst. Liq. Cryst.* **1973**, *1973*, 233. (b) Pugh, C.; Percec, V. *Polym. Bull.* **1990**, *23*, 177. (c) Viney, C.; Twieg, R. J.; Dannels, C. M.; Chang, M. Y. *Mol. Cryst. Liq. Cryst. Lett.* **1990**, *7*, 147. (d) Nguyen, P.; Lesley, G.; Dai, C.; Taylor, N. J.; Marder, T. B.; Chu, V.; Viney, C.; Ledoux, I.; Zyss, J. In *Applications of Organometallic Chemistry in the Preparation and Processing of Advanced Materials*; Harrod, J. F., Laine, R. M., Eds.; Kluwer Academic Publishers: Dordrecht, The Netherlands, 1995; p 333.

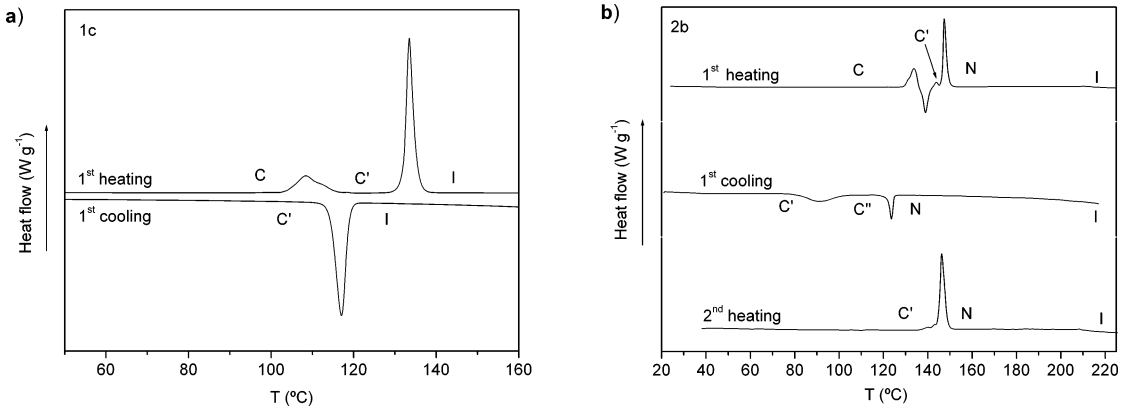


**Figure 1.** DSC curves (a) for compound **1c** and (b) for compound **2b**.

anthracene core. Compound **2a** shows a nematic mesophase with a relatively low aspect ratio ($L/D = 4.3$). An increase of the flexible part with the decyloxycarbonyl group (compound **2b**) makes polymorphism appear and lowers the melting and clearing points in the same extension. The as-obtained compound exhibits yellow color (C phase) at low temperatures, which transforms into orange crystals (C′ phase) after a complex transition involving melting and a cold recrystallization (Figure 1b). At 147 °C the solid melts to the nematic phase, in which marbled and Schlieren textures were observed under polarized light, until the isotropization occurs at 209 °C. The mesophase stability could be explained by the nonsymmetric substitution of the hard core. An X-ray diffraction pattern of **2b** performed at the temperature of the mesophase (150 °C) shows the usual features for a conventional nematic phase. It contains two diffuse maxima at low and high angles that correspond to mass−density fluctuations of 38.5 and 4.6 Å, respectively. The latter is typically observed for all kinds of liquid crystal phases and arises from short-range lateral interactions between the aromatic units and between the conformationally disordered hydrocarbon chains. The former maximum is relatively close to the molecular length estimated from Dreiding stereomodels (44 Å) and thus it is related to a density wave along the main molecular axis. This maximum can be assigned to the existence of short-range layer fluctuations in the nematic mesophase. No other features are detected in the X-ray pattern that could be related to the unusual molecule shape. On the DSC cooling cycle the nematic phase crystallizes as an unstable red solid (C″) that transforms into the orange C′ phase as deduced from the second heating cycle. The last transition could be also observed at the optical microscope. In summary, the as-obtained solid (C, yellow) transforms to another polymorph (C′, orange) after thermal treatment.

On increasing the length of the hard core with one more aromatic ring (compound **3a**) the transition temperatures rise and the nematic phase range is shorter. An exchange of an aromatic ring by a cyclohexane ring (compound **3b**) does not modify the transition temperatures but makes polymorphism appear, with a crystal-to-crystal transition at 126 °C involving a color change from yellow-orange to red-brown. Both compounds decompose over 270 °C as detected by a large exothermic peak at the DSC.

**Table 2. Absorption and Emission Data of the BPEA Derivatives in $CHCl_3$**

| compound | $\lambda$abs (log $\epsilon$) | $\lambda$em (exc 440 nm) | $\Phi_F$ |
|---|---|---|---|
| BPEA | 438 (4.51), 461 (4.53) | 475, 506 | 0.71[15] |
| **1a** | 451 (4.55), 472 (4.55) | 491, 521 | 0.61 |
| **1b** | 455 (4.61), 476 (4.59) | 496, 526$^{sh}$ | 0.66 |
| **1c** | 453 (4.63), 478 (4.62) | 489, 523 | 0.68 |
| **2a** | 455 (4.64), 474 (4.62) | 493, 524 | 0.66 |
| **2b** | 456 (4.66), 478 (4.64) | 494, 526 | 0.70 |
| **3a** | 456 (4.67), 477 (4.64) | 494, 526 | 0.75 |
| **3b** | 451 (4.60), 472 (4.59) | 488, 520 | 0.65 |

From all these data we can conclude that elongation of the BPEA skeleton with one aromatic ring (Series **2**) is crucial to induce mesomorphism. Size- and shape-dependent hard interactions are playing an important role in the appearance of the nematic phase in these systems.

**3.2 Spectroscopic Features.** The absorption spectra of all BPEA derivatives synthesized show two bands in chloroform solution (Table 2) around 455 and 475 nm, with a shoulder at 435 nm. A red-shift of 15 nm is observed with respect to the BPEA itself. Donor−acceptor substitution induces, in general, a slight bathochromic shift and an increase of the absorptivity (**1b** vs **1a**, **2b** vs **2a**).

All compounds are highly luminescent in solution (Table 2). The emission spectra of diluted solutions ($10^{-7}$ to $10^{-8}$ M) display two peaks: a sharp one in the blue-green region (495 nm) and a weaker one in the green region (525 nm) that make these compounds show an intense green fluorescence. All the spectra are quite similar, shifted to the green region compared to BPEA, and there is a slight bathochromic shift produced by the donor−acceptor substitution as in the absorption spectra. Quantum yields have been measured in chloroform relative to BPEA[15] showing that efficiency is comparable to this standard.

As it has been outlined in the thermal properties section, compounds **1b**, **1c**, **2b**, and **3b** show thermochromism related to thermal transitions as seen by DSC. IR spectra of the different crystals in KBr pellets show differences in the C≡C stretching band and/or the C═O stretching band related to the phase changes. For example, an IR study of compound **1c** at different temperatures shows a shift to lower frequencies in the C≡C and C═O stretching band passing from the low-temperature sample (r.t., C phase, red 2200, 1721 $cm^{-1}$) to the high-temperature sample (122 °C, C′ phase,

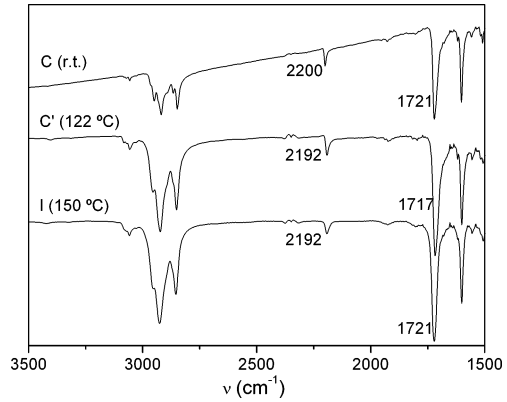


**Figure 2.** IR spectra of compound **1c** at different temperatures.

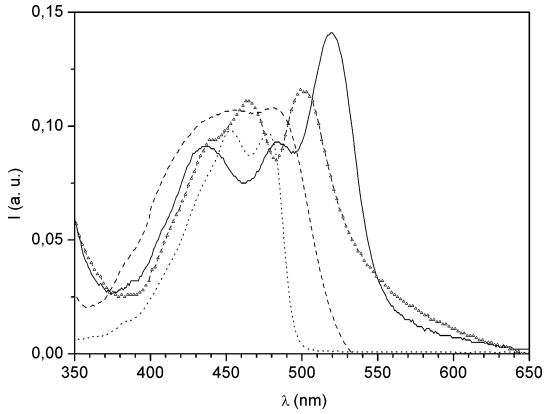


**Figure 3.** UV-vis spectra of compound **1c**: (—) red polymorph C; (△) yellow polymorph C′; (- -) isotropic liquid I; (•••) chloroform solution.

yellow 2192, 1717 $cm^{-1}$) and a recovery of the C═O stretching band on passing to the isotropic liquid (150 °C, I phase, 2192, 1721 $cm^{-1}$) (Figure 2). These changes indicate that different conformations of the molecules along the unsaturated bridges or the ester groups could be involved in the phase transitions.

Solid-state UV−vis spectra of compound **1c** in its red polymorph exhibit peaks at 438, 484, and 520 nm (Figure 3). The two last peaks shift 36 nm to the blue when the solid transforms into the yellow polymorph and the peak at 438 nm remains unchanged so they appear at 438, 464, and 501 nm. If pressure is applied to the yellow solid it turns red as it is observed by bare eye and by UV−vis spectroscopy and remains in this phase upon standing. This is in accordance with the previous thermal study which showed that the yellow polymorph was not thermodynamically stable. Bands at 520 and 500 nm are assigned as solid-state bands and belong to crystal packings with different degrees of intermolecular electronic interactions, as neither the solution nor the isotropic liquid (which are orange-red in color) display such bands. Therefore, the thermochromism in compound **1c** may arise from (failing single-crystal X-ray structures) the change from a crystalline arrangement with strong $\pi$-stacking (red) to another one (yellow) with a different and weaker overlap of adjacent rings that may occur as consequence of a change in the molecular conformation as it has been reported for other compounds with similar spectroscopic features.[17,18]

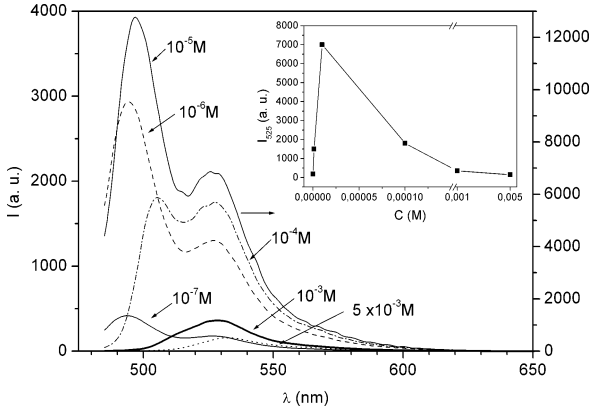


**Figure 4.** Fluorescence spectra of compound **2b** at different molar concentrations ($CHCl_3$, r.t.). Excitation wavelength 470 nm. Inset: Change of the intensity of the emission at 525 nm on increasing concentrations.

We have also studied in more detail compound **2b** in solution and in solid state as this compound displays the lowest temperature for the nematic phase. The compound does not aggregate in solution, as UV−vis spectra performed at different concentrations in chloroform show the same features in a wide range ($10^{-7}$ to $10^{-3}$ M). On the other hand, addition of a nonsolvent (methanol) in different amounts to chloroform solutions with the same total concentration did not induce aggregation effects because no extra peaks were detected. Only a slight hipsochromic shift (3−5 nm) took place, and in mixtures with 70% of methanol content the compound precipitated out as a yellow solid but soluble aggregates were not detected in the absorbance spectra of the compound.

Steady-state luminescence spectra show differences depending on the concentration. In high diluted solutions ($10^{-7}$ to $10^{-6}$ M) two maxima appear at 494 and 526 nm (higher intensity for the first peak), on increasing concentrations a gradual bathochromic shift of the low-wavelength peak and a decrease of its intensity with respect to the high-wavelength peak are observed, appearing as a shoulder of the high-wavelength peak in the spectrum of concentration $10^{-3}$ M and disappearing at higher concentrations (Figure 4). Moreover, the fluorescence intensity increases with concentration up to $10^{-5}$ M and decreases at higher concentrations, which can be explained by self-absorption of the emitted light. The emission band centered at 526 nm does not shift substantially when comparing the different curves, therefore single molecule emission is taking place in all cases and the decrease of the fluorescence intensity is due to the inner filter effect.

A film of 1% **2b** in a PMMA matrix shows an absorption spectrum similar to solution, and green fluorescence, with maxima similar to the solution spectra found for concentrated solutions of $10^{-4}$ to $10^{-3}$ M where self-absorption takes place. The molecules in the film are, therefore, not aggregated (Figure 5).

Solid-state UV−vis spectra of compound **2b** in the yellow (C) and orange (C′) polymorphs are similar and

(17) Tanaka, M.; Hayashi, H.; Matsumoto, S.; Casino, S.; Mogi, K. *Bull. Soc. Chem. Jpn.* **1997**, *70*, 329.
(18) (a) Aihara, J.; Kushibi, G.; Matsunaga, Y. *Bull. Soc. Chem. Jpn.* **1973**, *46*, 3584. (b) Desiraju, G. R.; Paul, I. C.; Curtin, D. Y. *J. Am. Chem. Soc.* **1977**, *99*, 4.

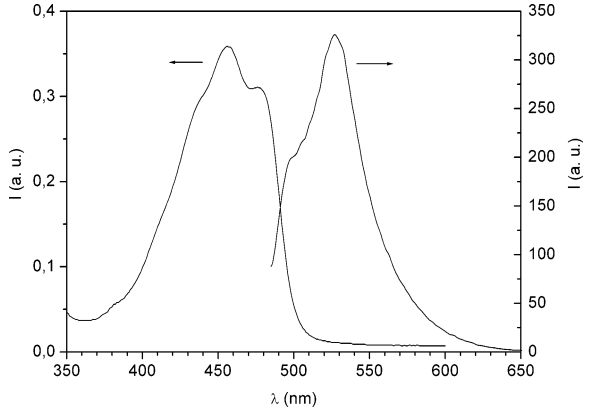


**Figure 5.** Absorbance and fluorescence spectra of a PMMA film containing 1% w/w of **2b**.

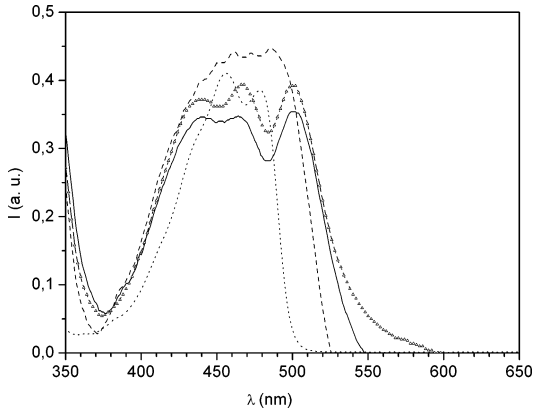


**Figure 6.** UV-vis spectra of compound **2b**: (—) orange polymorph C′; (△) yellow polymorph C; (- -) nematic phase N; (···) chloroform solution.

differ only in the relative intensity of the bands (Figure 6). The red polymorph (C″) is expected to have a red-shifted spectrum, but we were unable to study it as this polymorph is not stable at room temperature and all manipulations conducted on the samples in order to detect a nonsaturated spectrum at high temperature yielded the same bands as for C or C′ phases (439, 467, and 500 nm). In the mesophase, the absorption maximum shifts to lower wavelengths with a behavior similar to that found for the yellow solid and isotropic liquid of compound **1c**.

The crystal phase C′ of **2b** at room temperature shows a yellow-orange fluorescence that shifts to higher wavelengths when it melts to the nematic phase. This fluorescence remains in the isotropic liquid where some decomposition occurs, quenching the fluorescence gradually. The red-shift is typical of the formation of excited dimers (excimers).[19] A decrease of the intensity of the fluorescence with increasing temperature can also be oberved, which is generally expected for thermally activated radiationless processes (Figure 7).

Preliminary studies of the dichroic properties of these compounds have been performed to evaluate the potential applications for these materials. In particular, compound **2a** in a nematic mixture of low-molecular-weight LC displays a higher degree of order than BPEA ($S$ = 0.68 vs 0.52).[20−21] Moreover, **2a** exhibits higher photostability than BPEA (by a factor of 4) in PMMA films.[20] Both results place this anisotropic compound and analogous compounds as improved materials for applications in which oriented luminophores are required.

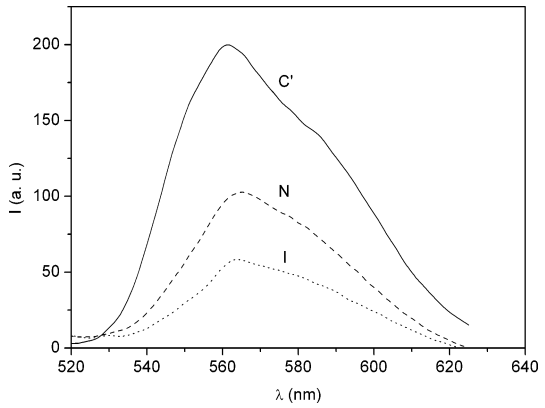


**Figure 7.** Fluorescence spectra of compound **2b** in pure state at different temperatures (C, crystal phase at r.t.; N, nematic phase at 180 °C; I, isotropic liquid at 220 °C). Excitation wavelength 470 nm.

## 4. Conclusions and Outlook

In conclusion, the extension of the BPEA chromophore along its long axis and the selection of adequate substituents seems to be a suitable approach to materials with improved dichroism, nematic mesomorphism at reasonable temperatures without decomposition, and efficient green emission in solution and at very low concentrations in polymeric matrixes. All these features make them interesting candidates to be included in emissive devices. Preparation of derived BPEA-containing materials with the adequate functionalization to be incorporated in side-chain polymers and study of the optical properties of oriented films are in progress.

**Acknowledgment.** We thank Prof. J. Barberá for performing XRD experiments in the mesophase, and Prof. J. Stumpe, R. Rosenhauer, Th. Fischer, Dr. E. Poetsch, and Prof. D. J. Broer for helpful discussions. We also thank Merck Co. for their generous gifts of chemicals. This work has been supported by the EC project BRPR-CT97-0485, the CICYT projects MAT2000-1293-CO2-01 and MAT2002-04118-CO2-02 from the Ministerio de Ciencia y Tecnología (Spain) and FEDER funds, and the Government of Aragón (D.G.A).

CM030582U

(19) (a) Stevens, B.; Ban; M. I. *Trans. Faraday Soc.* **1964**, *60*, 1515. (b) Jenekhe, S. A.; Osaheni, J. A. *Science* **1994**, *265*, 765.

(20) Rosenhauer, R.; Fischer, Th.; Stumpe, J.; Giménez, R.; Piñol, M.; Serrano, J. L.; Broer, D. *Proc. SPIE* **2002**, *4799*, 121.

(21) The degree of order of the films ($S$) has been calculated from the measured absorbance perpendicular (A) and parallel (A′) to the electric field vector of the incident light by the following equation: $S = (A - A')/(A + 2A')$.